



WRF-SBM Numerical Simulation of Aerosol Effects on Stratiform Warm Clouds in Jiangxi, China

Yi Li^{1,2}, Xiaoli Liu^{1,2*}, Hengjia Cai^{1,2}

¹ China Meteorological Administration Aerosol-Cloud and Precipitation Key Laboratory, Nanjing University of Information Science and Technology, Nanjing 210044, China.

² College of Atmospheric Physics, Nanjing University of Information Science and Technology, Nanjing 210044, China.

Correspondence to: Xiaoli Liu (liuxiaoli2004y@nuist.edu.cn)

Abstract. Aerosols, as cloud condensation nuclei (CCN), impact cloud droplet spectrum and dispersion (ϵ), affecting precipitation and climate change. However, the influence of various aerosol modes on cloud physics remains controversial, and this effect varies with geographical location and cloud type. This study uses a bin microphysics scheme (WRF-SBM) to simulate a warm stratiform cloud in the Jiangxi region of China. The numerical simulations reproduce the macro and microstructure of warm clouds compared with aircraft observations. Further experiments modifying the aerosol spectrum and number concentration indicate: increased aerosol concentration promotes cloud formation, raises cloud height, and broadens the cloud droplet spectrum. In contrast, a decrease in aerosol concentration suppresses cloud formation and development. Different aerosols have varying effects on the cloud droplet spectrum. Accumulation mode aerosols increase small droplet concentration, while nucleation and coarse mode aerosols favor the production of large droplets. Generally, the correlation between ϵ and volume-weighted particle size (rv) changes from positive to negative as rv increases. The transition in correlation is influenced by the relative strengths of cloud droplet collision, condensation, and activation processes. The increase in accumulation mode aerosol concentration strengthens the positive correlation between ϵ and rv in the rv range of 4.5-8 μm , while the decrease in concentration strengthens the negative correlation in the same range. Regardless of different coalescence intensity, ϵ converges with the increase in N_c . Changes in aerosol concentration for different modes do not alter the convergence trend of ϵ - N_c but only affect the dispersion of ϵ at low N_c levels.

1 Introduction

According to Lau and Wu (2003), warm clouds account for 32% of total precipitation in tropical regions and cover 72% of the total precipitation area. Warm clouds play a critical role in evaluating cloud-precipitation-climate feedback, making understanding their formation, development, and cloud microphysical processes a crucial topic in cloud physics (Zhao and Ishizaka, 2004; Seifert and Onishi, 2010).

In previous studies on warm clouds, many researchers have focused on changes in cloud characteristics such as number concentration or particle size (Grosvenor et al., 2018; Zheng et al., 2021). However, these studies have overlooked the impact of changes in particle size distribution in clouds, which may be critical for parameterizing cloud droplet effective



radius and is an essential factor that cannot be ignored during cloud-rain auto-conversion processes, affecting macroscopic and microscopic physical processes in clouds (Lu et al., 2022; Xie et al., 2015).

Cloud droplet spectral relative dispersion (ϵ) is an important parameter that describes the width and distribution of cloud droplet sizes. It is represented as the ratio between the standard deviation (σ) and the mean radius (r_{ave}) of the droplets
35 (Wang and Lu, 2022). On the one hand, dispersion influences the effective radius of cloud droplets and the auto-conversion, thereby affecting cloud precipitation processes (Liu et al., 2005, 2006; Zhu et al., 2020; Lu and Xu, 2021; Wang et al., 2022 ; Wang et al., 2023; Yang et al., 2023). On the other hand, dispersion affects cloud-aerosol interactions, impacting macroclimate (Xie et al., 2017)

However, as Lu et al. (2020) summarized, existing studies on cloud droplet spectrum correlations primarily rely on
40 empirical data from observations, leading to significant uncertainty in characterizing the ϵ within clouds. On the one hand, the relationship between the ϵ and the volume-mean radius (r_v) has shown varied conclusions in different studies: some indicate a negative correlation (Liu et al., 2008; Pandithurai et al., 2012), while others suggest a positive correlation (Tas et al., 2012). Additionally, some research has found that as r_v increases, the ϵ exhibits a converging trend (Chen et al., 2016). Furthermore, the correlation between the ϵ and cloud droplet number concentration (N_c) also shows uncertainty. Some
45 studies report a positive correlation (Pandithurai et al., 2012; Chen et al., 2016), while others indicate a negative correlation (Cecchini et al., 2017; Wang et al., 2011). Some studies even suggest that no significant correlation is observed between ϵ and N_c (Tas et al., 2015).

Numerous researchers have conducted causal analyses of its variations in response to the uncertainty surrounding the distribution characteristics of ϵ . The results indicate that the variability of ϵ is influenced by various factors, such as
50 atmospheric temperature, humidity, and entrainment (Lu et al., 2013). Zhu et al. (2020) found that in adiabatic clouds, vertical velocity plays a dominant role, and an increase in vertical velocity promotes the activation of cloud condensation nuclei (CCN), leading to an increase in N_c and facilitating droplet coalescence and growth. On the other hand, Kumar et al. (2017) showed that ϵ is also related to turbulent mixing and variations in vertical velocity within the cloud.

In recent years, studies by Ma et al. (2010), Wang et al. (2011, 2019), and others have shown that changes in ϵ are
55 highly sensitive to aerosol concentration and its activation process. Additionally, alterations in aerosol concentration or size distribution significantly impact the cloud-rain auto-conversion process through ϵ changes. Consequently, ϵ becomes a critical link connecting aerosol-cloud-rain auto-conversion processes (Liu and Daum, 2002).

Currently, some studies suggest that an increase in aerosol concentration leads to a reduction in ϵ , thereby inhibiting the cloud-rain auto-conversion process (Chandrakar et al., 2016, 2018; Desai et al., 2019). For example, Liu et al. (2003)
60 compared aircraft observations and satellite retrievals for warm clouds in both the northern and southern hemispheres and found that an increase in aerosol concentration leads to a decrease in cloud droplet effective radius and narrowing of the droplet spectrum, thus suppressing warm precipitation processes. Yang et al. (2017) analyzed aerosol concentration and cloud droplet spectrum distribution in the high-altitude region of eastern China during summer. The experimental results showed that increased aerosol concentration inhibits the cloud-rain auto-conversion process, resulting in more cloud water



65 remaining in the atmosphere and reducing warm precipitation. Kant et al. (2019) analyzed aerosol observations in India from 2000 to 2017. They found that strong updrafts with abundant mineral dust aerosols can activate more cloud droplets, leading to competition for water vapor and narrowing the droplet spectrum, limiting the growth of high-level liquid droplets.

However, there are also studies indicating that an increase in aerosol concentration results in an increase in ϵ and enhances droplet collision and coalescence processes (Yum and Hudson, 2005; Rotstajn and Liu, 2003; Rotstajn and Liu, 70 2009; Prabha et al., 2012). For instance, Liu et al. (2020) found that increasing aerosol concentration in clean tropical or marine regions can prolong cloud lifetimes and enhance precipitation by modifying the cloud droplet spectrum distribution. Moreover, it is observed that the influence of aerosol concentration changes on cloud droplet size distribution exhibits strong regional dependence and varies according to cloud types and geographical regions, as corroborated by Chandraka et al. (2016, 2018), who conducted sensitivity experiments using bubble models and reached similar conclusions.

75 In addition, the impact of aerosol concentration changes on cloud droplet spectrum varies at different size ranges. Liu et al. (2022), using satellite data to investigate the influence of aerosols on warm cloud processes, found that fine particles with diameters ranging from 0.1 to 2.5 micrometers, acting as cloud condensation nuclei, can suppress precipitation and prolong the lifetime of maritime warm clouds, like the conclusions of Kovačević (2018) and Lerach and Cotton (2018). On the other hand, an increase in coarse-mode marine condensation nuclei with larger particle sizes leads to a noticeable increase in cloud 80 droplet effective radius and warm rain intensity. Studies by Yin et al. (2000) and Jensen and Nugent (2017) revealed that large particles with diameters exceeding 2 micrometers, acting as giant cloud condensation nuclei, can increase ϵ and facilitate cloud droplet growth during the collision-coalescence process. However, Wehbe et al. (2020) analyzed aircraft observations over the United Arab Emirates in 2019. It is found that although giant cloud condensation nuclei were present, no significant collision-coalescence process was observed in warm clouds.

85 Furthermore, Rosenfeld et al. (2001) attributed the reduction in cloud droplet effective radius over the Sahara Desert to numerous submicron-sized cloud condensation nuclei (CCN), which decreased ϵ exacerbated the decrease in precipitation over the Sahara region. Numerical experiments by Flossmann and Wobrock (2010) yielded similar conclusions.

In summary, the changes in aerosol physicochemical properties under the climate change background significantly impact the microphysical characteristics of warm clouds. However, the response patterns of warm clouds to aerosol 90 physicochemical properties are regions and cloud types dependently, making this issue an essential yet controversial scientific question in climate prediction. Existing studies have mainly explored the effects of aerosols on warm cloud microphysical properties by examining changes in aerosol concentration, CCN, and N_c . Considering that different types of aerosols act as CCN and influence cloud droplet nucleation, leading to variations in warm cloud microphysical characteristics differently, it is essential to investigate further the impact of aerosol spectrum changes on warm cloud 95 processes.

This study uses the Weather Research and Forecasting (WRF) model with the SBM-FAST bin microphysics scheme to simulate a warm cloud event in Jiangxi, China. Numerical experiments are conducted to explore the effects of changes in nucleation, accumulation, coarse, and total mode aerosol concentrations on the macro and micro characteristics of warm



clouds in Jiangxi, China. The aim is to provide more background support for numerical simulations of warm clouds and the
100 study of cloud droplet spectrum characteristics in the East China region.

2 Simulation Setup and Experimental Design

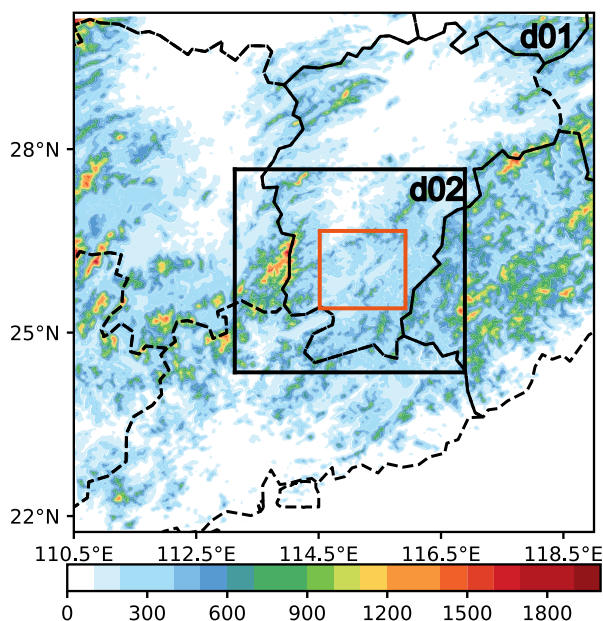
2.1 Simulation Setup and Weather Conditions

This paper selects a warm cloud process that occurred in the Jiangxi region on December 25, 2014, and conducts simulations
using the WRF (Weather Research and Forecasting) 4.2 version. The experiment comprises one control group and five
105 aerosol spectrum modification experimental groups. Apart from aerosol concentrations, all groups keep the initial field data
and simulation settings consistent. The simulations use the Fifth generation of ECMWF atmospheric reanalyzes of the global
climate (ERA5) hourly data on pressure levels as the initial field, with a resolution of $0.25^{\circ} \times 0.25^{\circ}$.

The simulations adopt a two-layer nesting approach, with grid resolutions of 3 km and 1 km, and the innermost layer
grid is 376×376 . The microphysics scheme used is the new version SBM-fast bin scheme (FSBM-2) under the WRF 4.2
110 version. The boundary layer scheme selected is the Mellor-Yamada-Janjic (Eta) Turbulence Kinetic Energy (TKE) scheme,
and the near-surface layer scheme uses the Monin-Obukhov (Janjic Eta) scheme. The land surface process adopts the unified
Noah land-surface model. The (old) Goddard shortwave radiation scheme is used, and the Rapid Radiative Transfer Model
(RRTM) scheme is chosen for longwave radiation.

The simulation region is illustrated in Fig. 1, The simulation period is from 18:00 on December 24, 2014, to 06:00 on
115 December 25, 2014 (UTC), and no precipitation was observed at the ground during the simulation period. The simulated
area, Ganzhou City, Jiangxi Province, is in the southern part of eastern China's Jiangxi Province. It is located upstream of the
Gan River and in the transitional zone between the southeastern coastal and central inland regions. The city is surrounded by
mountains and faulted basins traverse through Ganzhou. The predominant topographical features are mountains, hills, and
basins. The area is located at the southern edge of the subtropical zone and falls under the subtropical monsoon climate
120 region.

As shown in Fig. 2, at 00:00 on the 25th, a high-altitude trough shifted eastward, with the mid-level located in the
southwest jet stream, which was relatively weak. At the 850hPa level, there was wind shear with relatively low shear wind
speeds, and the ascent situation was relatively gentle.



125 **Figure 1: The simulated range is shown in the figure. The shading represents the elevation (m) of the terrain, and the area within the red box is the analysis range.**

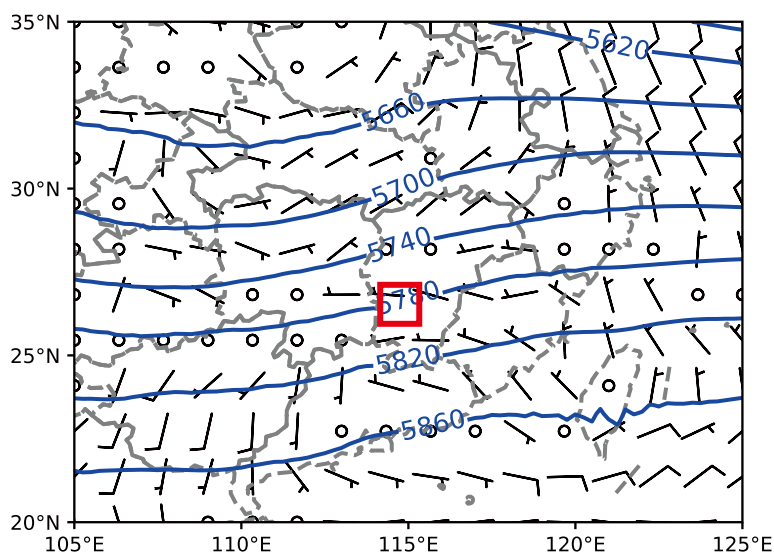


Figure 2: At 00:00 (UTC) on December 25, 2014, the 500 hPa geopotential height field (blue contour lines, unit: dagpm) and the 700 hPa wind field (wind barbs) are shown. the area within the red box indicates the starting point of the flight.

130 2.2 Introduction to Microphysics Scheme

The SBM-fast scheme was initially developed by Khain and Lynn (2009) as a simplified version of the SBM-full bin scheme based on the original microphysics scheme included in the Hebrew University Cloud Model (HUCM) (FSBM-1) (Khain and



Sednev, 1996; Khain et al., 2000). The FSBM-2 used in this study is an improvement over FSBM-1 by Shpund et al. (2019) and has been verified to exhibit better simulation performance (Han et al., 2019).

135 In FSBM-2, cloud and rain droplets are described using a unified liquid droplet bin scheme, which is divided into 33 bins. The aerosol scheme is divided into marine and continental components, and the aerosol spectrum distribution is described using 43 or 33 mass bins. Regardless of whether 33 or 43 aerosol bins are used, the maximum dry aerosol radius is set to 2 μm . The scheme activates aerosols into liquid droplets under supersaturated conditions (cloud nucleation: Pinsky and Khain, 2018). In the model, the minimum CCN size is assumed to be 0.003 μm , and the initial aerosol distribution is
140 represented by the sum of three lognormal distributions, corresponding to the nucleation mode (centered at 0.008 μm), accumulation mode (centered at 0.034 μm), and coarse mode (centered at 0.46 μm). The grid-based solution for nucleation in clouds is computed using supersaturation, and the algorithm's accuracy is verified through comparison with large-eddy simulation results (Iltoviz et al., 2015).

2.3 Sensitivity Experiment Configuration

145 This paper includes five aerosol concentration modification experiments and one control experiment (ORG). The initial aerosol concentrations are set in the control experiment, as shown in Table 1. The initial aerosol concentrations are set for the other experimental groups that modify the initial aerosol spectrum, as shown in Table 2. Experiments 1, 2, and 3, respectively, modify the aerosol concentrations of the nucleation mode (NM), accumulation mode (AM), and coarse mode (CM) to five times their original values. Experiment 4 (ITM) simultaneously modifies the aerosol concentrations of the
150 nucleation, accumulation, and coarse modes to five times their original values. Experiment 5 (DTM) reduces the aerosol concentrations by five times compared to the original group. After the simulations, the initial aerosol spectrum information in the analysis area is shown in Fig. 3.

Table 1: Initial Aerosol Concentration in the Control Experiment.

Aerosol Types	Number Concentration ($/\text{cm}^{-3}$)	Mean Particle Size (μm)
Nucleation Mode	1000.000	0.008
Accumulation Mode	800.000	0.034
Coarse Mode	0.720	0.460

155

Table 2: Initial Aerosol Concentration Settings in the Experimental Groups.

	Nucleation Mode ($/\text{cm}^{-3}$)	Accumulation Mode ($/\text{cm}^{-3}$)	Coarse Mode ($/\text{cm}^{-3}$)
Experiment 1 (NM)	5000.000	800.000	0.720
Experiment 2 (AM)	1000.000	4000.000	0.720



Experiment 3 (CM)	1000.000	800.000	3.600
Experiment 4 (ITM)	5000.000	4000.000	3.600
Experiment5 (DTM)	200.000	160.000	0.144

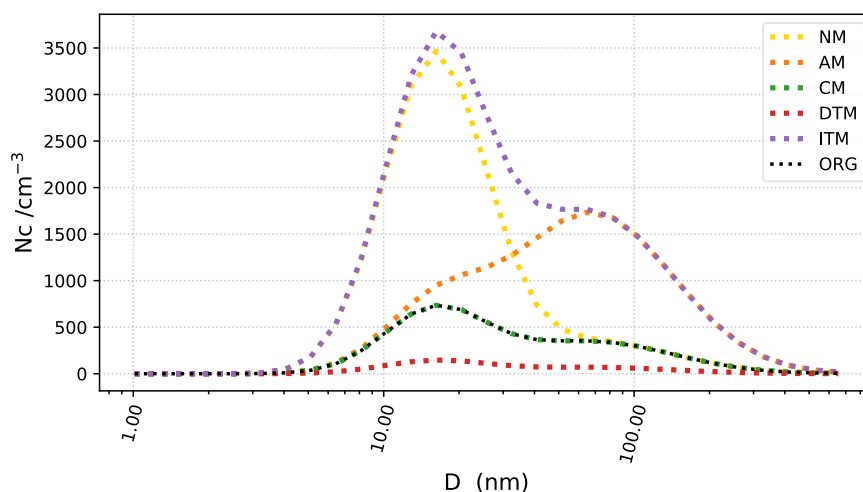


Figure 3: Initial aerosol number concentration (unit: /cm³) as a function of particle diameters (unit: nm).

160 2.4 Calculation of Cloud Droplet Spectrum Parameters

In this study, the changes in cloud droplet spectrum and cloud droplet spectral parameters were analyzed. The average cloud droplet diameter (D), cloud droplet volume-weighted radius (r_v), cloud-rain auto-conversion threshold (T), cloud droplet spectral relative dispersion (ϵ), and cloud droplet activation intensity (FBS) were calculated as shown in Supplement.

3 Results and analysis

165 3.1 Simulation Results Validation

To verify the simulation performance of the control experiment, we compared the simulated results with cloud-top temperature observations from the FY2G satellite and aircraft observations on December 25, 2014. The results are shown in Fig. 5 and Fig. 6. The satellite data was obtained from the National Meteorological Science Data Center, and it represents the 1-hour cloud-top temperature product observed by the FY2G satellite's VISSR instrument.

170 Figure 5 shows that the control experiment and satellite data both show band-like warm cloud regions with cloud-top temperatures ranging from 5 to 10°C in the central and northern parts of Jiangxi. The distribution of observed and simulated cloud-top temperatures is quite similar.

Aircraft observation data on December 25, 2014, in the Jiangxi region were chosen to further validate the simulated vertical distribution of cloud microphysical characteristics. The data was obtained from the CAS probe onboard the aircraft,



175 which measures aerosols and cloud particles with diameters ranging from 0.51 to 50 μm , covering 30 bins with varying size bins. The observation period was from 01:35 to 4:45 (UTC) on December 25, 2014. The observed cloud region within the area covered by the aircraft had a maximum horizontal extent of more than 50 km and was characterized as a stratiform warm cloud process. For the control experiment, the cloud water content, cloud droplet number concentration, and average cloud droplet diameter were compared in the same observation duration and flight regions.

180 Figure 6 shows that both the control experiment and the observation show an increase followed by a decrease in cloud water content with height. Regarding number concentration of cloud droplet, there are some differences in the vertical variation trend between the two groups. Still, the magnitudes of the number concentrations of the control experiment and the observation are generally consistent. Additionally, the average particle size in both groups increases with height, and their vertical distribution trends are consistent.

185 Overall, regarding the distribution of warm clouds and the vertical distribution of cloud microphysical properties, the simulation results are generally consistent with the observed data. Therefore, the simulation results are reliable.

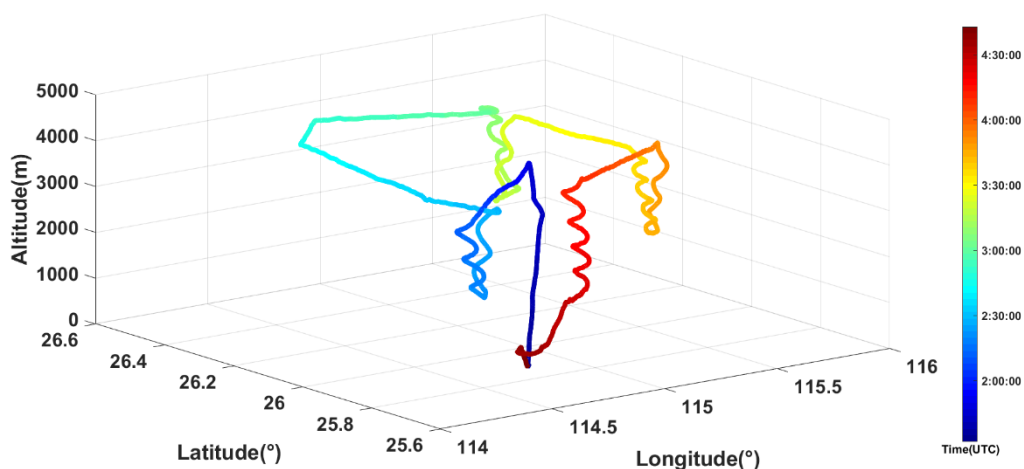
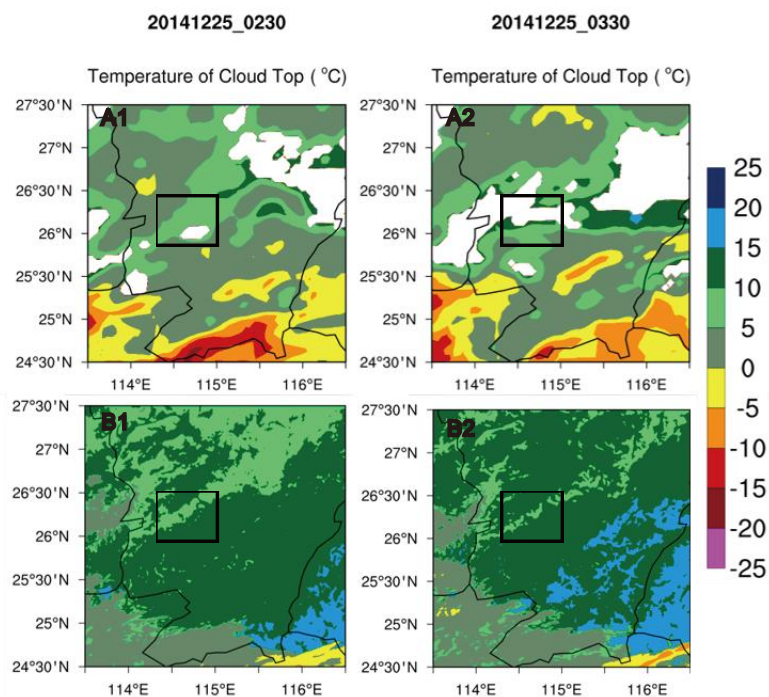


Figure 4: The flight track of the observing aircraft on December 25, 2014, with the line colors representing the flight time.



190 **Figure 5: On December 25, 2014, at 02:30 (A1) and 03:30 (B1), FY2G observed cloud-top temperature. At 02:30 (A2) and 03:30 (B2), simulated cloud-top temperature of the control experiment (unit: °C). The black box in the figure indicates the aircraft observation area.**

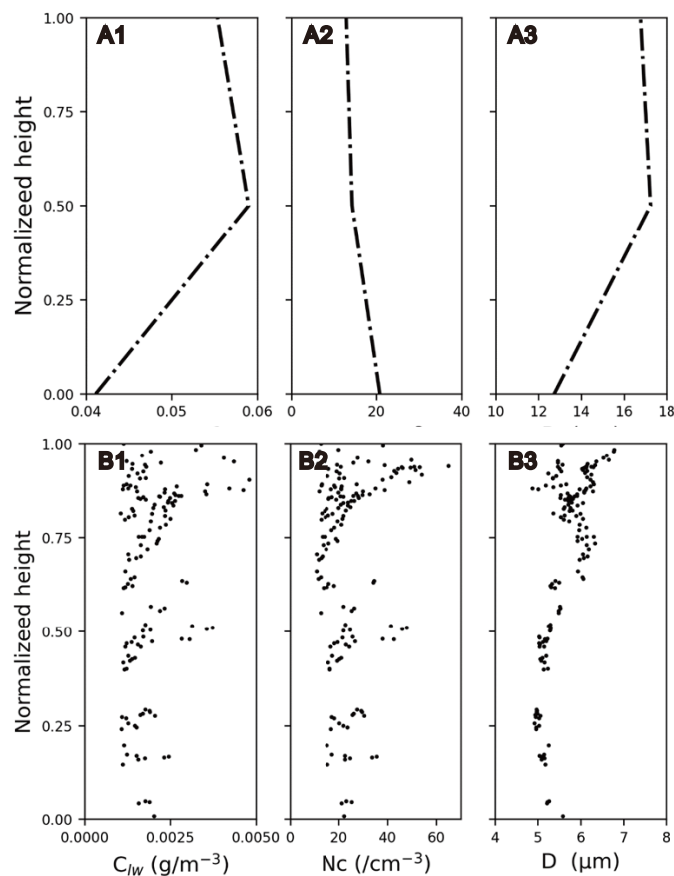


Figure 6: Vertical distribution of domanian and temporal averaged water content (unit: g/m^3), cloud droplet number concentration (unit: cm^{-3}), and cloud droplet diameter (unit: μm) from 00:00 to 05:00 (UTC) on December 25, 2014. (Ai) represents aircraft observations, and (Bi) represents the control experiments; 1, 2, and 3 represent water content, number concentration, and cloud droplet average diameter, respectively.

195

3.2 Analysis of the Impact of Background Aerosols on Warm Cloud Properties

3.2.1 Vertical Distribution of Cloud Microphysical Properties

200

Figure 7 reflects that the cloud thickness significantly increases as the cloud system develops. The variations in liquid water content of cloud droplet (C_{lw}) and D show high consistency. In the early stages of the process, both C_{lw} and D decrease with height before increasing at later stages. Conversely, the N_c exhibits a decreasing trend with height. Large numbers of small cloud droplets present at the cloud base, the primary area for droplet activation. The peak of C_{lw} appears at higher cloud layers. In contrast, the maximum cloud droplet diameter occurs in the middle to upper cloud layers, indicating that the main region of increased cloud droplet size is near the top and middle-upper cloud regions.

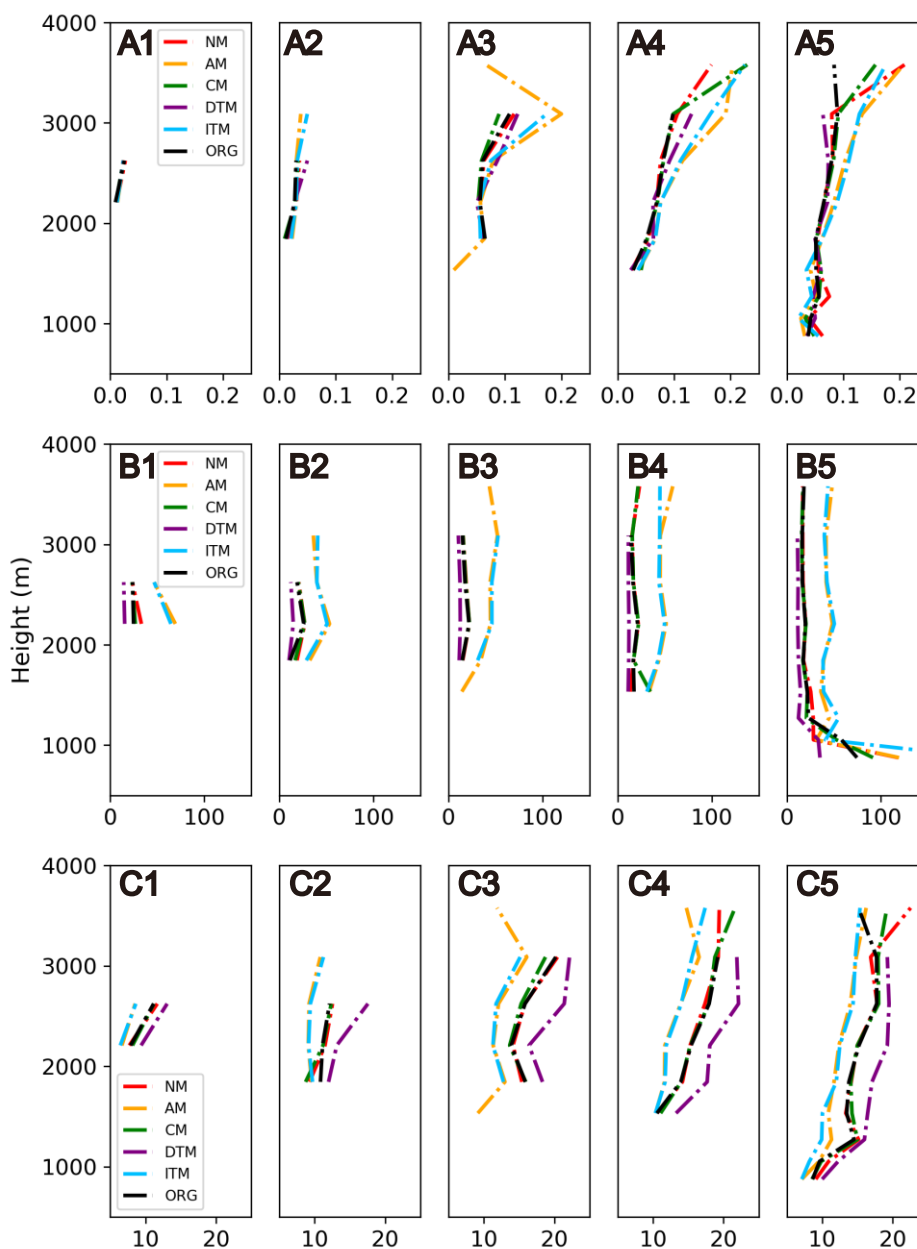
205

Compared to the control experiment, the increase in aerosol concentration promotes cloud development and raises cloud-top height. This phenomenon is consistent with the findings of Khain et al. (2005) and Morrison et al. (2018). When



the accumulation mode aerosol concentration increases, this "promoting" effect becomes most evident. On the other hand, when aerosol concentration decreases, cloud development is suppressed, resulting in a noticeable decrease in cloud-top
210 height.

In terms of cloud microphysical properties, with an increase in aerosol concentration, N_c noticeably increases. As a result, more small cloud droplets compete for water vapor, reducing cloud droplet size. The maximum N_c and minimum cloud droplet size are observed in the ITM and AM experiments. However, when aerosol concentration decreases, despite cloud development being restrained, the DTM experiment exhibits the largest cloud droplet size.



215

Figure 7: Hourly variations of (A) cloud droplet liquid water content (Cl_w) (unit: g/cm^3), (B) cloud droplet number concentration (N_c) (unit: cm^{-3}), and (C) average cloud droplet diameter (D) as a function of altitude. And 1, 2, 3, 4, and 5 correspond to 01:00, 02:00, 03:00, 04:00, and 05:00 (UTC) on the 25th.

3.2.2 Cloud Droplet Size Distribution

220 Based on the analysis in the preceding text, cloud microphysical properties exhibit three distinct variation intervals concerning vertical height: below 1500m, between 1500m and 3000m, and above 3000m. Therefore, dividing these three



height intervals allows for analyzing different variations in cloud droplet spectrum distribution, as shown in Fig. 8. As particle size increases, N_c decreases exponentially in different height intervals. However, with increasing altitude, the concentration of large-size cloud droplets with diameters above 28 micrometers increase. In the AM experiment, there is a notable increase in cloud droplets with sizes between 4 and 20 micrometers. On the other hand, in the NM and CM experiments, the percentage of large droplets with sizes between 30 and 50 micrometers is the highest.

Figure 9 represents the hourly probability distribution of N_c concerning D . As the cloud system develops, the cloud droplet spectrum widens and exhibits a unimodal distribution. When aerosol concentration increases, the cloud droplet spectrum broadens earlier, and the maximum N_c appears in the AM and ITM experiments. Additionally, the peak of the droplet spectrum differs among the experiments. The AM and ITM experiments have their peaks in the 9-15 micrometer size range, while the NM and CM experiments have their peaks concentrated in the 15-24 micrometer size range. After aerosol concentration decreases in the DTM experiment, a tendency of spectrum broadening is observed. However, the spectrum width is smaller than in the control experiment, and the N_c is lower.

This analysis shows that increased aerosol concentration promotes cloud development and leads to an earlier widening of the cloud droplet spectrum. The increase in accumulation mode aerosols tends to increase the number concentration of small-sized cloud droplets. In contrast, an increase in nucleation and coarse mode aerosols favors the production of large-sized cloud droplets. In the NM experiment, although the particle size of nucleation mode aerosols is small, the increase in aerosol concentration still leads to an increase in cloud droplet number concentration because aerosol particle sizes follow a normal distribution in the WRF-SBM scheme. Therefore, aerosol particles with larger sizes within the nucleation mode range can still participate in cloud droplet activation.

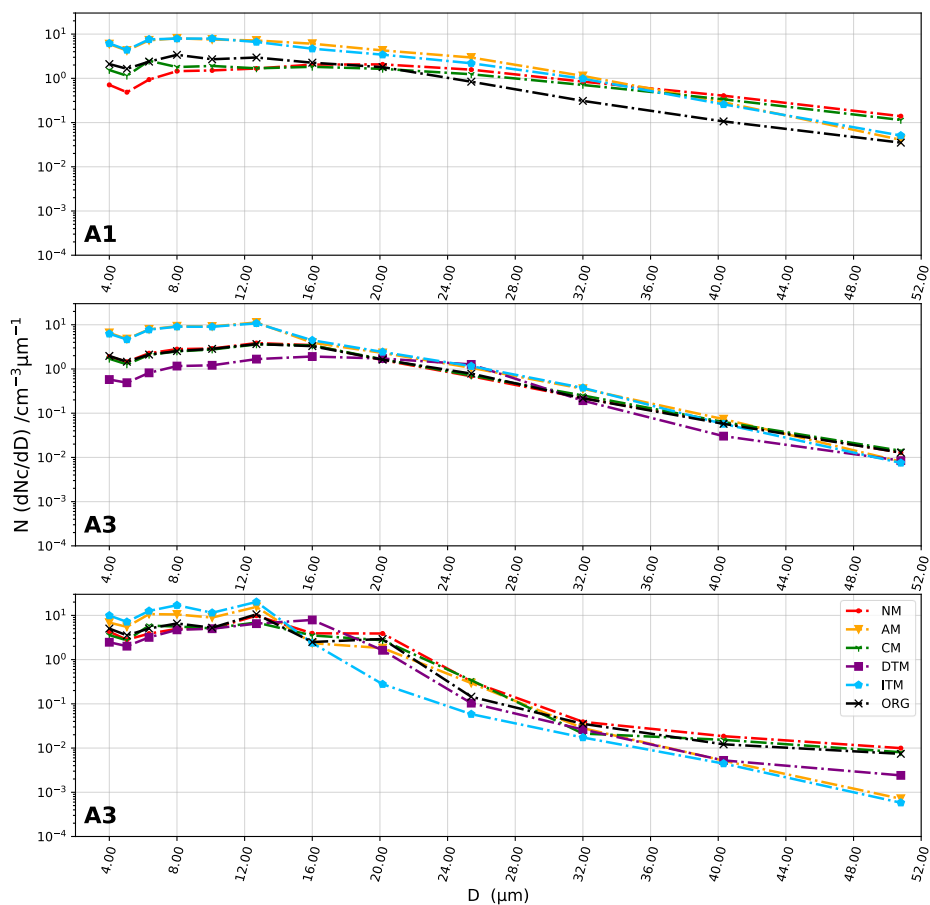
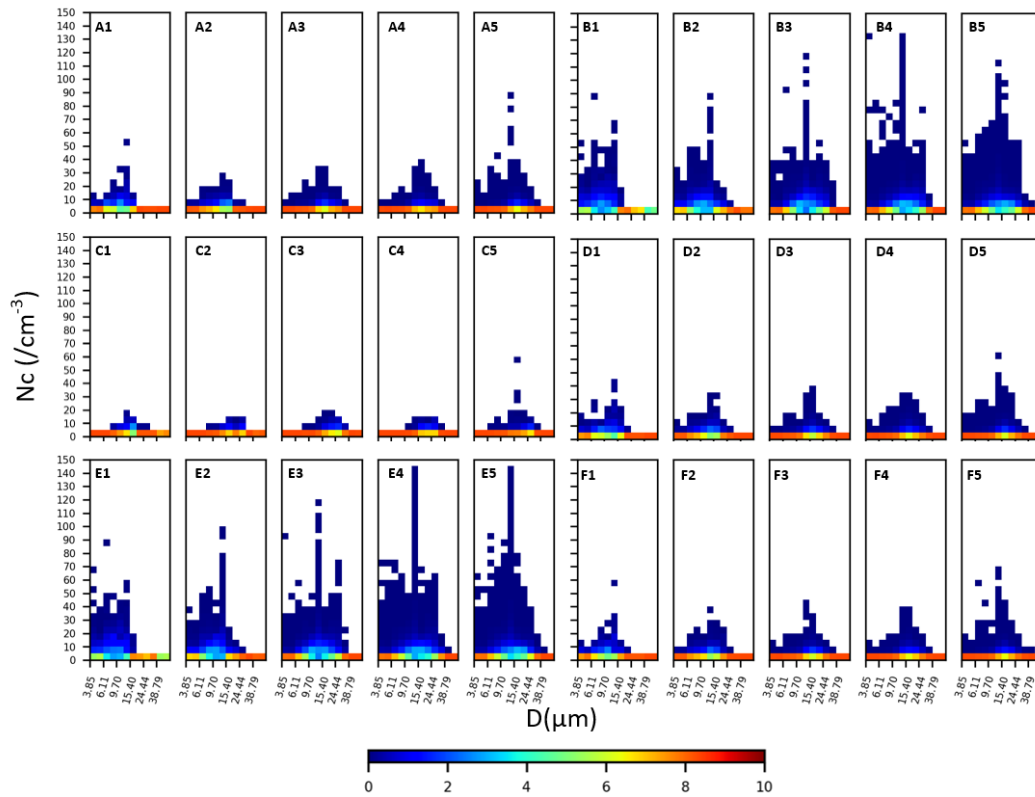


Figure 8: Cloud droplet size distributions above 3000m (A1), between 1500m and 3000m (A2), and below 1500m (A3). D represents the average cloud droplet diameter (unit: μm).



245 **Figure 9: The probability distribution of cloud droplet average number concentration N_c (unit: /cm³) with respect to the mean diameter D (unit: μm), where A, B, C, D, E, and F represent ORG, ITM, DTM, NM, AM, CM experiments, and 1, 2, 3, 4, 5 represent 01:00, 02:00, 03:00, 04:00, 05:00 on the 25th. The shading represents the probability magnitude.**

3.3 Analysis of Cloud Droplet Spectrum Characteristics

3.3.1 Vertical profiles of cloud droplet spectrum characteristics

250 To analyze the impact of aerosols on cloud droplet spectrum and cloud microphysical processes, Fig. 10 was given out to illustrate the variations of hourly ε , cloud-rain auto-conversion intensity (T), and r_v with altitude. The T value represents the probability of auto-conversion occurrence, which can be used to assess the intensity of collision and coalescence processes during cloud and precipitation (Liu et al., 2005, 2006). In the early stages of the process, the collision and coalescence intensity within the cloud is low, and T value decreases with altitude and then increases. The trend of r_v with altitude is

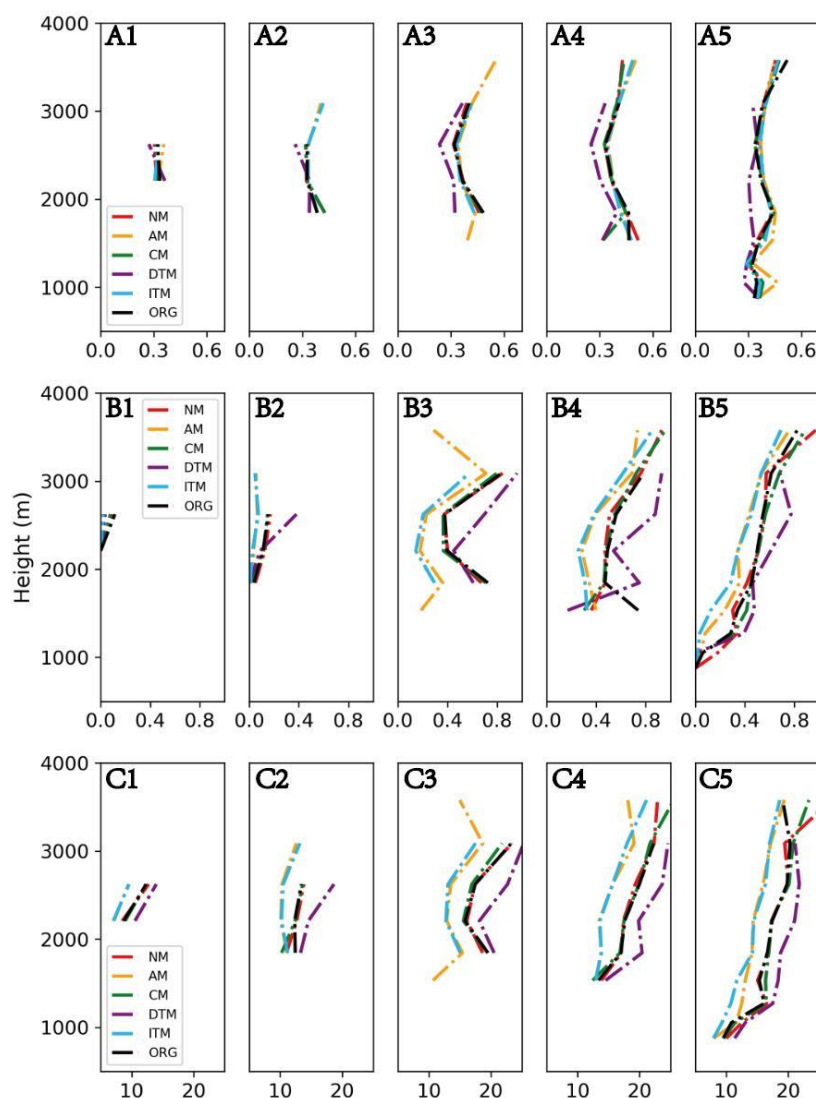
255 consistent with the T value during this stage, indicating that the cloud droplet collision and coalescence growth mainly occur at the cloud base and top. On later stage of the process, the collision and coalescence processes within the cloud gradually strengthen and show an increasing trend with altitude. The intense collision and coalescence regions with T values > 0.5 are primarily located in the middle to upper parts of the cloud, consistent with the distribution trend of r_v with altitude.

ε represents the relative degree of particle dispersion in cloud droplets, which defined as the ratio of standard deviation of droplet radius to mean droplet radius of droplet size distributions. From Fig. 10, it can be observed that the dispersion

260

does not monotonically change with r_v or T . As the T value increases, the dispersion shows a trend from increasing to decreasing with altitude, ultimately converging within the range of 0.3-0.4.

265 Compared to the control experiment, the ITM and AM experiments have significantly smaller r_v values, resulting in smaller cloud droplet sizes and lower collision and coalescence intensities than the other experiments. When the aerosol concentration decreases, the r_v in the DTM experiment increases, leading to higher collision and coalescence intensity than the other experiments. Additionally, fewer small cloud droplets are activated due to the lower aerosol concentration in the DTM experiment, resulting in lower dispersion than the other experiments.



270 **Figure 10: Hourly average cloud droplet spectral relative dispersion (ϵ) (A), cloud droplet collision and coalescence intensity (T) (B), and cloud droplet volume-weighted radius (r_v) (unit: μm) (C) as a function of altitude. The values 1, 2, 3, 4, and 5 represent 01:00, 02:00, 03:00, 04:00, and 05:00 on the 25th.**



3.3.2 Relationship between ε - r_v

As shown in Fig. 11, ε does not vary monotonically with r_v . There is a significant difference in cloud droplet collision and coalescence intensity around 8 μm radius of cloud droplet. When the r_v is smaller than 8 μm , cloud droplet growth mainly depends on the condensation process. At this stage, there exists a critical radius r_c (4.2 μm). When $r_v < 4.2\mu\text{m}$, ε shows a positive correlation with r_v , while when $r_v > 4.2\mu\text{m}$, ε shows a negative correlation with r_v . This trend is like the study by Lu et al. (2020), but the value of r_c differs. In the experiments, increased aerosol concentration enhances the positive correlation between ε and r_v . In the ITM and AM experiments, the negative correlation trend changes to a positive one when $r_v > 4.2\mu\text{m}$. In contrast, decreasing aerosol concentration strengthens the negative correlation trend between ε and r_v .

In the range of r_v larger than 8 μm , collision and coalescence intensity increase with the cloud droplet size, and cloud droplet growth mainly relies on the collision and coalescence process. At this stage, ε decreases with r_v , but it exhibits an overall converging trend, with the convergence interval close to 0.2-0.4.

Lu et al. (2020) pointed out that the change in the correlation between ε and r_v is related to the interaction between the condensation/coalescence and activation (evaporation and deactivation) processes. Therefore, to further investigate the causes of the correlation change, Fig. 12 presents the correlation between r_v and N_c .

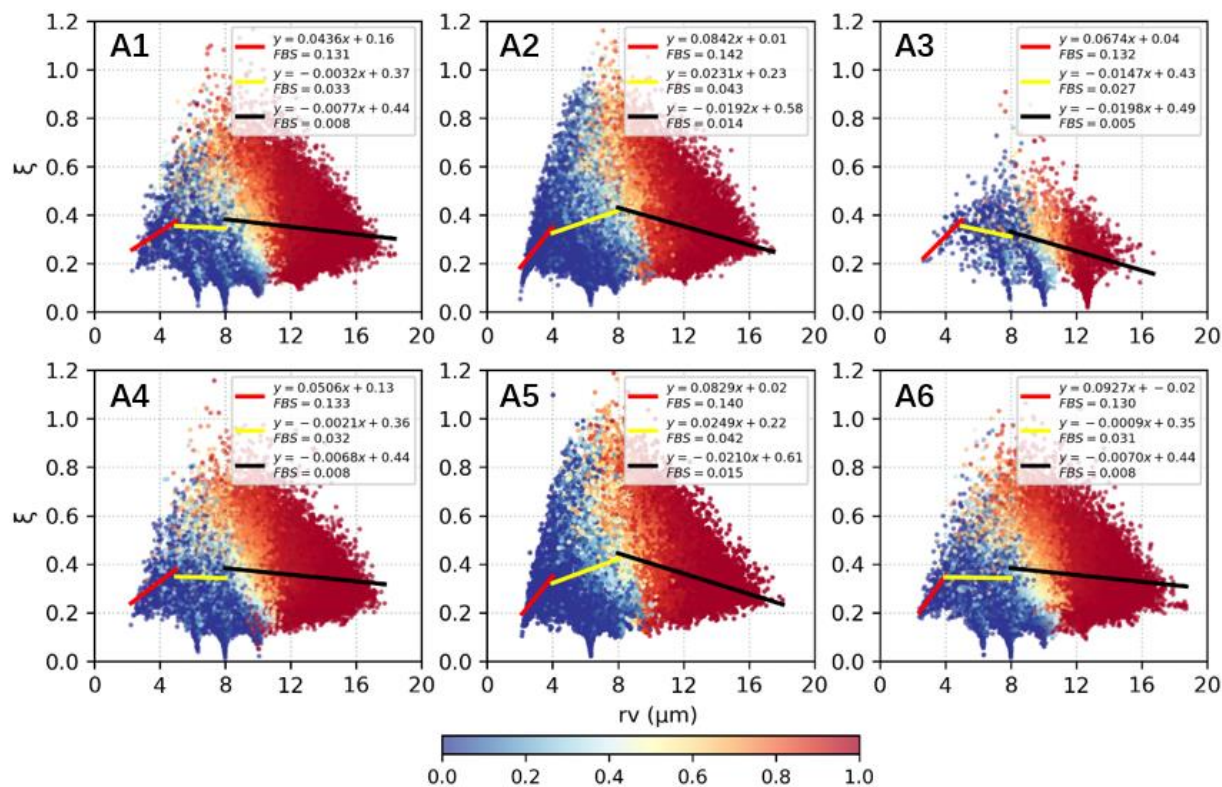
In the 2-8 μm range, cloud droplets primarily grow through condensation. When $r_v < 4.2\mu\text{m}$, the activation of cloud droplets is active, and activation and condensation growth coincide. N_c increases with r_v , and ε shows a positive correlation with r_v . When $r_v > 4.2\mu\text{m}$, the activation intensity of cloud droplets decreases, and the coalescence process has not yet started. At this point, N_c shows no significant variation in particle size. Due to the decreased efficiency of condensation growth with increasing particle size, small-sized cloud droplets proliferate through condensation, while larger-sized cloud droplets grow more slowly. As r_v increases, ε shows a negative correlation with r_v , and cloud droplet particles tend to become monodisperse, resulting in a narrower cloud droplet spectrum. This finding is like the results of Liu et al. (2006) and Peng et al. (2007). When r_v exceeds 8 μm , the ε converges as r_v increases, ultimately approaching the range of 0.3-0.4, consistent with Lu et al. (2020).

In the experiments, an increase in aerosol concentration enhances the activation intensity of cloud droplets, enhancing the positive correlation between ε and r_v . Among different aerosol types, an increase in accumulation mode aerosol contributes to the prolonged maintenance of cloud droplet activation. When $r_v > 4.2\mu\text{m}$, ε shows a positive correlation with r_v . However, when cloud droplet size increases above 8 μm , cloud droplet coalescence intensity increases with particle size, while cloud droplet number concentration decreases as r_v increases. Therefore, when cloud droplet coalescence is the dominant process with weak activation intensity, cloud droplet coalescence promotes the rapid growth of cloud droplet size, increasing large-sized cloud droplets while simultaneously consuming small-sized cloud droplets. As a result, ε tends to converge with particle size.

In addition, during the analysis in Fig. 12, it is shown that the correlation between N_c and cloud microphysical processes is more complex. Regions with the same N_c may be dominated by condensation growth or coalescence processes.



305 Furthermore, the ε -Nc correlation, which is significantly influenced by activation, condensation, and coalescence processes, may exhibit even more complex variations. Therefore, in Fig. 13, we explore the ε -Nc correlation.



310 **Figure 11:** The cloud droplet spectral relative dispersion (ε) is plotted against the cloud droplet volume-weighted radius (rv , in μm) for different experiments, including A1, A2, A3, A4, A5, and A6, representing ORG, ITM, DTM, NM, AM, and CM experiments, respectively. FBS indicates the cloud droplet activation intensity, and the shading represents the coalescence intensity.

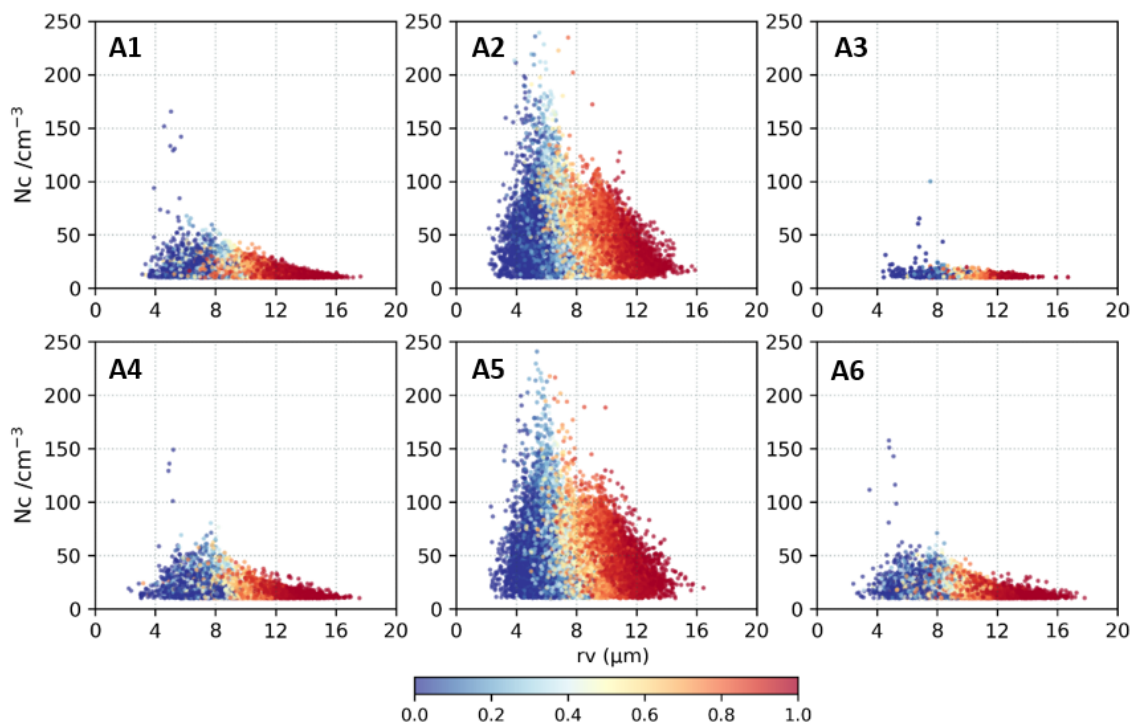
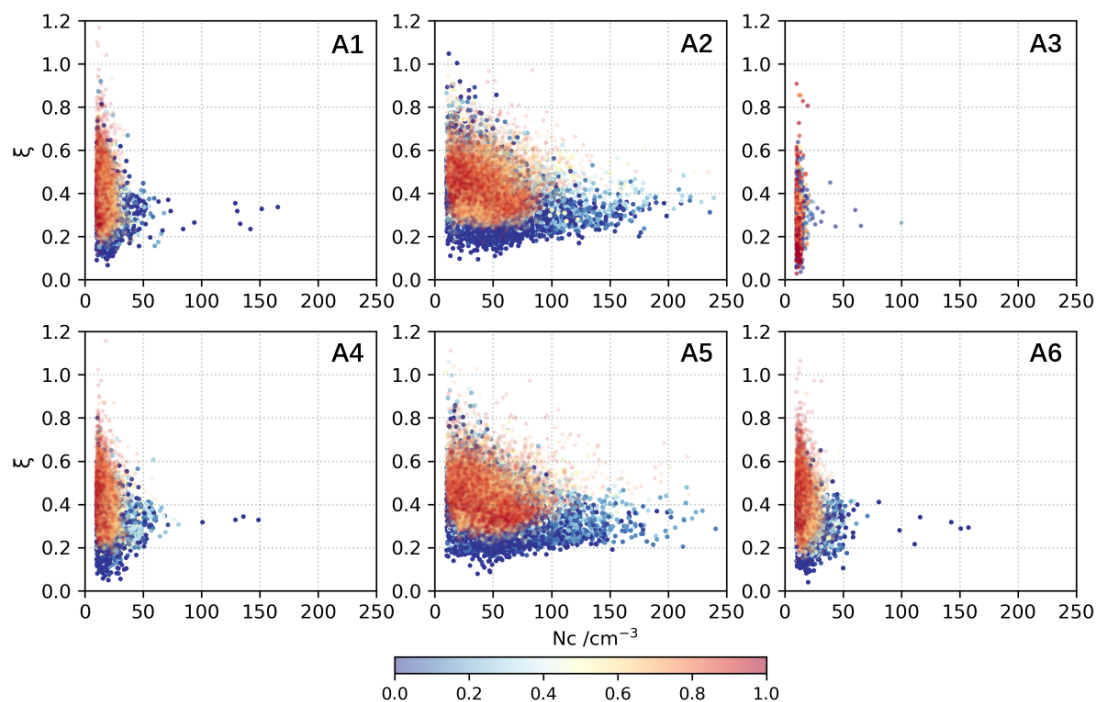


Figure 12: The cloud droplet number concentration (N_c , in cm^{-3}) is plotted against the cloud droplet volume-weighted radius (r_v , in μm) for different experiments, including A1, A2, A3, A4, A5, and A6, representing ORG, ITM, DTM, NM, AM, and CM experiments, respectively. The shading represents the coalescence intensity.

315 3.3.3 Relationship between ε - N_c

As shown in Fig. 13, as N_c increases, ε tends to converge, consistent with the findings of Zhao et al. (2006) and Jin et al. (2022). Additionally, the coalescence intensity does not significantly impact the ε - N_c correlation. With increased coalescence intensity, the dispersion of ε in the low N_c region decreases, but the ε - N_c relationship still shows a converging trend.

320 Compared to the control experiment, changes in aerosol concentration did not affect the ε - N_c correlation. When the aerosol concentration increased, N_c significantly increased, and in the AM and ITM experiments, the dispersion of ε slightly increased in the low coalescence intensity region. On the other hand, a decrease in aerosol concentration led to a significant reduction in N_c and increased cloud droplet size. In the region with $T > 0.8$, the dispersion of ε was higher.



325 **Figure 13: The cloud droplet spectral relative dispersion (ϵ) varies with cloud droplet number concentration (N_c) (unit: cm^{-3}). The experiments A1, A2, A3, A4, A5, and A6 represent the ORG, ITM, DTM, NM, AM, and CM experiments, respectively. The shading represents the coalescence intensity.**

4 Discussion

The study of ϵ has been a focus of cloud microphysics over the past 20 years. However, the responses of warm clouds to aerosol physicochemical properties vary in different regions and cloud characteristics, leading to some controversies regarding the impact of aerosols on warm cloud microphysics (Desai et al., 2019).

335 Firstly, different aerosol modes have varying effects on warm cloud processes. Liu et al. (2022) used satellite observations to analyze the impact of aerosols on warm cloud processes. They found that fine particles with diameters in the range of 0.1-2.5 micrometers, acting as cloud condensation nuclei, would suppress precipitation and prolong the lifespan of maritime warm clouds. On the other hand, the increase of coarse-mode sea salt condensation nuclei with larger diameters led to a significant increase in cloud droplet effective radius and warm rain intensity. In this study, the increase of coarse-mode aerosol concentration resulted in the enlargement of r_v and enhanced collision-coalescence intensity, consistent with Liu et al. (2022). However, in this study, the increase in nucleation-mode particles also contributed to more vigorous cloud development, with significantly larger r_v and collision-coalescence intensity than the control experiment. This difference may arise from variations in cloud height and cloud water content.

340



Furthermore, the relationship between ε and cloud microphysical properties differs from previous studies. In this study, ε shows a convergence trend as N_c increases, and the variation in aerosol concentration does not change this trend but rather affects the degree of dispersion, which is like the conclusions of Deng et al. (2009) and Yu et al. (2018). In contrast, Ma et al. (2010) studied non-precipitating stratiform clouds in North China using aircraft observation data. They found that with an increase in aerosol concentration, ε tends to decrease with increasing N_c , while Anil et al. (2016) found the opposite trend, with ε showing a positive correlation with N_c .

The complex variations in ε - N_c correlation are mainly due to the sensitivity of N_c and ε to many microphysical processes, such as updraft strength, aerosol properties, or condensation-coalescence processes (Lu et al., 2012; Peng et al., 2007). As shown in Fig. 7 and Fig. 8, it is difficult to determine the corresponding relationship between N_c and cloud microphysical processes during the fitting process of ε - N_c correlation. In regions with low N_c , it may correspond to the strong collision/coalescence initiation zone, while in regions with higher N_c , it may simultaneously be in the condensation/coalescence dominant zone. As stated by Liu et al. (2008) and Tas et al. (2012), compared to N_c , r_v considers the synergistic relationship between N_c and water content, providing a more explicit mapping to cloud microphysical processes. Therefore, this study analyzes the ε - r_v correlation to provide a more systematic understanding of the research on stratiform warm clouds in East China.

5 Conclusions

This study used the SBM-FAST bin scheme in the WRF model to simulate a warm cloud process in Jiangxi, China. Numerical experiments were further conducted to investigate the impact of changes in nucleation mode, accumulation mode, coarse mode, and total aerosol concentrations on the macroscopic and microscopic characteristics of warm clouds. The variations in cloud microphysical parameters with aerosol concentrations were analyzed, the ε - r_v and ε - N_c relationships were fitted to explore the influence of microphysical processes on ε . Specific conclusions are as follows:

(1) The numerical simulation with bin microphysics scheme reproduces warm clouds' macro- and microscopic characteristics in Jiangxi, China. As the cloud system develops, r_v and T values gradually increase. Vertically, r_v increases with height, and T strengthens synchronously with the enlargement of cloud droplet size. The relationship between the variable ε and T values or r_v is not strictly monotonous. ε initially rises with increasing T values, followed by a subsequent decline before converging around 0.3. Furthermore, it is observed that variations in aerosol concentrations exert a significant influence on cloud development. With an increase in the aerosol concentration of any mode, the cloud droplet spectrum widens earlier. Specifically, higher aerosol concentrations promote cloud growth, increasing cloud-top height. In comparison, lower aerosol concentrations impede cloud droplet activation, decreasing the concentration of cloud droplets and leading to a notable reduction in ε and increased r_v and higher T values.

(2) In contrast, different modes of aerosol concentration variations impact cloud microphysical properties differently. An increase in accumulation mode aerosol tends to increase the concentration of small-size cloud droplets, leading to



decreased r_v and a lower collision and coalescence intensity concerning the control experiment. An increase in nucleation mode and coarse mode aerosols favors the production of large cloud droplets. As a result, the increase in accumulation mode aerosol has the most significant impact on N_c enhancement. On the other hand, increases in nucleation mode and coarse mode aerosol concentrations result in an increase in r_v and an enhancement of collision and coalescence intensity.

(3) The variation of ε in the cloud is closely related to cloud microphysical processes. Fitting the ε with r_v and N_c reveals that as r_v increases, the correlation between ε and r_v changes from positive to negative, eventually converging. This transformation is mainly related to cloud droplet activation, condensation, and collision-coalescence processes within the cloud. When T values are less than 0.5, as cloud droplet condensation growth becomes more active and nucleation weakens, the cloud droplet spectrum dispersion transitions from an increasing trend to a decreasing trend with the increase in r_v . With the enhanced coalescence between cloud droplets, ε primarily decreases with the increase in r_v . Increasing accumulation mode aerosol concentration contributes to the prolonged cloud droplet activation, enhancing the positive correlation trend between ε and r_v . On the other hand, a decrease in aerosol concentration leads to a reduction in cloud droplet activation intensity, making the negative correlation trend between ε and r_v more pronounced. In addition, regardless of different T values, ε converges with the increase in N_c . As N_c increases, ε converges to a range of 0.2-0.4. Changes in aerosol concentration for different modes do not alter the converging trend of ε with N_c but only affect the dispersion degree of ε at low N_c values.

6 Conflict of Interest

The authors declare that the research was conducted in the absence of any commercial or financial relationships that could be construed as a potential conflict of interest.

7 Acknowledgments

In addition, we acknowledge the High Performance Computing Center of Nanjing University of Information Science and Technology for their support of this work.

8 Funding

This work was supported by the National Natural Science Foundation of China (Grant Nos. 42061134009 and 41975176) and 2023 Jiangsu Provincial College Students' Innovative Entrepreneurial Training Program (Grant Nos.202310300108Y).



9 Data Availability Statement

The data used in this study can be accessed at the following link: <https://doi.org/10.57760/sciencedb.11210>. The data link
400 includes the satellite-observed cloud top temperature data, WRF model simulation results, and simulated initial aerosol
spectrum information used in this study.

The cloud top temperature data used in this study is obtained from the China National Meteorological Science Data
Center. It represents the hourly cloud top temperature product observed by the VISSR instrument on the FY2G satellite. The
data format is .hdf, and the temporal resolution is 30 minutes.

405 The WRF model simulation configurations are described in the previous section. The data format is .netcdf, and details
about the data and its dimensions can be found in the data description.

The initial aerosol spectrum data includes the distribution information of aerosol spectra within the first hour of the
simulation for one control group and five experimental groups mentioned in the article. The temporal resolution is 10
minutes. Data details can be found in the data description.

410 In addition, the initial fields used in the numerical simulations are based on the Fifth generation of ECMWF
atmospheric reanalysis of the global climate (ERA5) hourly data on pressure levels. These data can be accessed at the
following link: <https://cds.climate.copernicus.eu/cdsapp#!/dataset/reanalysis-era5-pressure-levels?tab=overview>. The study
utilized all height variables for every 6 hours from December 24th, 2014, 18:00 to December 25th, 2014, 06:00.

If the manuscript is accepted, the data will be publicly available through the aforementioned link
415 (<https://doi.org/10.57760/sciencedb.11210>). To access the data, you only need to use the database link and provide your
name, affiliation, and purpose of the data request to the authors for download.

10 References

- Anil Kumar, V. et al.: Investigation of aerosol indirect effects on monsoon clouds using ground-based measurements over a
high-altitude site in Western Ghats, *Atmospheric Chemistry and Physics*, 16(13), pp. 8423–8430. doi:10.5194/acp-16-
420 8423-2016, 2016.
- Cecchini, M.A. et al.: Sensitivities of amazonian clouds to aerosols and updraft speed, *Atmospheric Chemistry and Physics*,
17(16), pp. 10037–10050. doi:10.5194/acp-17-10037-2017, 2017.
- Chandrakar, K.K. et al.: Aerosol indirect effect from turbulence-induced broadening of cloud-droplet size distributions,
Proceedings of the National Academy of Sciences, 113(50), pp. 14243–14248. doi:10.1073/pnas.1612686113, 2016.
- 425 Chandrakar, K.K., Cantrell, W. and Shaw, R.A.: Influence of turbulent fluctuations on cloud droplet size dispersion and
aerosol indirect effects, *Journal of the Atmospheric Sciences*, 75(9), pp. 3191–3209. doi:10.1175/jas-d-18-0006.1, 2018.
- Chen, J. et al.: New understanding and quantification of the regime dependence of aerosol-cloud interaction for studying
aerosol indirect effects, *Geophysical Research Letters*, 43(4), pp. 1780–1787. doi:10.1002/2016gl067683, 2016.



- Desai, N. et al.: Search for microphysical signatures of stochastic condensation in marine boundary layer clouds using
430 airborne digital holography, *Journal of Geophysical Research: Atmospheres*, 124(5), pp. 2739–2752.
doi:10.1029/2018jd029033, 2019.
- Flossmann, A.I. and Wobrock, W.: A review of our understanding of the aerosol–cloud interaction from the perspective of a
bin resolved cloud scale modellinm, *Atmospheric Research*, 97(4), pp. 478–497. doi:10.1016/j.atmosres.2010.05.008,
2010.
- 435 Grosvenor, D. P., Sourdeval, O., Zuidema, P., Ackerman, A., Alexandrov, M. D., Bennartz, R., et al.: Remote sensing of
droplet number concentration in warm clouds: A review of the current state of knowledge and perspectives. *Reviews of
Geophysics*, 56, 409– 453. <https://doi.org/10.1029/2017RG000593>, 2018.
- Han, B. et al.: Cloud-Resolving Model Intercomparison of an MC3E squall line case: Part II. Stratiform precipitation
properties, *Journal of Geophysical Research: Atmospheres*, 124(2), pp. 1090–1117. Available at:
440 <https://doi.org/10.1029/2018jd029596>, 2019.
- Hersbach, H., Bell, B., Berrisford, P., Biavati, G., Horányi, A., Muñoz Sabater, J., Nicolas, J., Peubey, C., Radu, R., Rozum,
I., Schepers, D., Simmons, A., Soci, C., Dee, D., Thépaut, J.-N.: ERA5 hourly data on pressure levels from 1940 to
present. Copernicus Climate Change Service (C3S) Climate Data Store (CDS), DOI: 10.24381/cds.bd0915c6, 2023.
- Ilotoviz, E. et al.: Effect of aerosols on freezing drops, hail, and precipitation in a midlatitude storm, *Journal of the
445 Atmospheric Sciences*, 73(1), pp. 109–144. doi:10.1175/jas-d-14-0155.1, 2015.
- Jensen, J.B. and Nugent, A.D.: Condensational growth of drops formed on giant sea-salt aerosol particles, *Journal of the
Atmospheric Sciences*, 74(3), pp. 679–697. doi:10.1175/jas-d-15-0370.1, 2017.
- JIN Yuchen, NIU Shengjie, LÜ Jingjing, et al.: Study of the Microphysical Structural Characteristics and Cloud–Rain
Autoconversion Threshold Function of Stratiform Warm Clouds in Jiangxi [J]. *Chinese Journal of Atmospheric
450 Sciences*, 45(5): 981–993. doi: 10.3878/j.issn.1006-9895.2102.20166, 2021.
- Kant, S., Panda, J. and Gautam, R.: A seasonal analysis of aerosol-cloud-radiation interaction over Indian region during
2000–2017, *Atmospheric Environment*, 201, pp. 212–222. doi:10.1016/j.atmosenv.2018.12.044, 2019.
- Khain, A. and Sednev, I.: Simulation of precipitation formation in the Eastern Mediterranean Coastal Zone using a spectral
microphysics cloud ensemble model, *Atmospheric Research*, 43(1), pp. 77–110. Available at:
455 [https://doi.org/10.1016/s0169-8095\(96\)00005-1](https://doi.org/10.1016/s0169-8095(96)00005-1), 1996.
- Khain, A. et al.: Notes on the state-of-the-art numerical modeling of Cloud Microphysics, *Atmospheric Research*, 55(3-4),
pp. 159–224. Available at: [https://doi.org/10.1016/s0169-8095\(00\)00064-8](https://doi.org/10.1016/s0169-8095(00)00064-8), 2000.
- Khain A P, Rosenfeld D, Pokrovsky A, et al.: Effects of Atmospheric Aerosols On Precipitation From Deep Convective
Clouds As Seen From Simulations Using A Spectral Microphysics Cloud Model[J]. Available at:
460 2002EGSGA.27.6326K, 2002.



- Khain, A., Rosenfeld, D. and Pokrovsky, A.: Aerosol impact on the dynamics and microphysics of deep convective clouds. *Quarterly Journal of the Royal Meteorological Society: A journal of the atmospheric sciences, applied meteorology and physical oceanography*, 131(611), pp.2639-2663, 2005.
- Khain, A. and Lynn, B.: Simulation of a supercell storm in clean and dirty atmosphere using weather research and forecast model with spectral bin Microphysics, *Journal of Geophysical Research*, 114(D19). Available at: <https://doi.org/10.1029/2009jd011827>, 2009.
- 465
- Kovačević, N.: Hail suppression effectiveness for varying solubility of natural aerosols in water, *Meteorology and Atmospheric Physics*, 131(3), pp. 585–599. doi:10.1007/s00703-018-0587-4, 2018.
- Kumar, B. et al.: Cloud-edge mixing: Direct numerical simulation and observations in Indian Monsoon clouds, *Journal of Advances in Modeling Earth Systems*, 9(1), pp. 332–353. doi:10.1002/2016ms000731, 2017.
- 470
- Lau, K.M. and Wu, H.T.: Warm rain processes over tropical oceans and climate implications, *Geophysical Research Letters*, 30(24). Available at: <https://doi.org/10.1029/2003gl018567>, 2003.
- Lerach, D.G. and Cotton, W.R.: Simulating southwestern U.S. desert dust influences on supercell thunderstorms, *Atmospheric Research*, 204, pp. 78–93. doi:10.1016/j.atmosres.2017.12.005, 2018.
- 475
- Liu, F. et al.: Opposing comparable large effects of fine aerosols and coarse sea spray on marine warm clouds, *Communications Earth & Environment*, 3(1). doi:10.1038/s43247-022-00562-y, 2022.
- Liu, G.: Retrieval of cloud droplet size from visible and microwave radiometric measurements during INDOEX: Implication to aerosols' indirect radiative effect, *Journal of Geophysical Research*, 108(D1). doi:10.1029/2001jd001395, 2003.
- Liu, Y. and Daum, P.H.: Indirect warming effect from dispersion forcing, *Nature*, 419(6907), pp. 580–581. doi:10.1038/419580a, 2002.
- 480
- Liu, Y.: Size truncation effect, threshold behavior, and a new type of autoconversion parameterization, *Geophysical Research Letters*, 32(11). doi:10.1029/2005gl022636, 2005.
- Liu, Y. et al.: Generalized threshold function accounting for effect of relative dispersion on threshold behavior of autoconversion process, *Geophysical Research Letters*, 33(11). doi:10.1029/2005gl025500, 2006.
- 485
- Liu, Y. et al.: Dispersion bias, dispersion effect, and the aerosol–cloud conundrum, *Environmental Research Letters*, 3(4), p. 045021. doi:10.1088/1748-9326/3/4/045021, 2008.
- Liu, Y. et al.: Tibetan Plateau driven impact of Taklimakan dust on northern rainfall, *Atmospheric Environment*, 234, p. 117583. doi:10.1016/j.atmosenv.2020.117583, 2020.
- Lu, C. et al.: Observed impacts of vertical velocity on cloud microphysics and implications for aerosol indirect effects, *Geophysical Research Letters*, 39(21). doi:10.1029/2012gl053599, 2012.
- 490
- Lu, C. et al.: Empirical relationship between entrainment rate and microphysics in cumulus clouds', *Geophysical Research Letters*, 40(10), pp. 2333–2338. doi:10.1002/grl.50445, 2013.
- Lu, C. et al.: Reconciling contrasting relationships between relative dispersion and volume-mean radius of cloud droplet size distributions, *Journal of Geophysical Research: Atmospheres*, 125(9). doi:10.1029/2019jd031868, 2020.



- 495 Lu, C. S., & Xu, X. Q.: Research Progress on Cloud Entrainment-Mixing Processes. *Torrential Rain and Disasters (in China)*,
40(3), 271-279. DOI: 10.3969/j.issn.1004-9045.2021.03.005, 2021.
- Ma, J. et al.: Strong air pollution causes widespread haze-clouds over China, *Journal of Geophysical Research*, 115(D18).
doi:10.1029/2009jd013065, 2010.
- Morrison, H. et al.: Broadening of modeled cloud droplet spectra using bin microphysics in an Eulerian spatial domain,
500 *Journal of the Atmospheric Sciences*, 75(11), pp. 4005–4030. doi:10.1175/jas-d-18-0055.1, 2018.
- Pandithurai, G. et al.: Aerosol effect on droplet spectral dispersion in warm continental cumuli, *Journal of Geophysical
Research: Atmospheres*, 117(D16). doi:10.1029/2011jd016532, 2012.
- Peng, Y. et al.: An investigation into the aerosol dispersion effect through the activation process in marine stratus clouds,
Journal of Geophysical Research, 112(D11). doi:10.1029/2006jd007401, 2007.
- 505 Pinsky, M. and Khain, A.: Theoretical Analysis of the Entrainment–mixing process at cloud boundaries. part I: Droplet size
distributions and humidity within the interface zone, *Journal of the Atmospheric Sciences*, 75(6), pp. 2049–2064.
doi:10.1175/jas-d-17-0308.1, 2018.
- Prabha, T.V. et al.: Spectral width of premonsoon and monsoon clouds over Indo-Gangetic Valley, *Journal of Geophysical
Research: Atmospheres*, 117(D20). doi:10.1029/2011jd016837, 2012.
- 510 Rosenfeld, D., Rudich, Y. and Lahav, R.: Desert dust suppressing precipitation: A possible desertification feedback loop,
Proceedings of the National Academy of Sciences, 98(11), pp. 5975–5980. doi:10.1073/pnas.101122798, 2001.
- Rotstajn, L.D. and Liu, Y.: Sensitivity of the first indirect aerosol effect to an increase of cloud droplet spectral dispersion
with droplet number concentration, *Journal of Climate*, 16(21), pp. 3476–3481. doi:10.1175/1520-
0442(2003)016<3476:sotfia>2.0.co;2, 2003.
- 515 Rotstajn, L.D. and Liu, Y.: Cloud droplet spectral dispersion and the indirect aerosol effect: Comparison of two treatments
in a GCM, *Geophysical Research Letters*, 36(10). doi:10.1029/2009gl038216, 2009.
- Seifert, A., Nuijens, L. and Stevens, B.: Turbulence effects on warm-rain autoconversion in precipitating shallow convection.
Quarterly Journal of the Royal Meteorological Society, 136(652), pp.1753-1762, 2010.
- Shpund, J. et al.: Simulating a mesoscale convective system using WRF with a new spectral bin Microphysics: 1: Hail vs
520 graupel, *Journal of Geophysical Research: Atmospheres*, 124(24), pp. 14072–14101. doi:10.1029/2019jd030576, 2019.
- Tas, E., Koren, I. and Altaratz, O.: On the sensitivity of droplet size relative dispersion to warm cumulus cloud evolution,
Geophysical Research Letters, 39(13). doi:10.1029/2012gl052157, 2012.
- Tas, E. et al.: The relative dispersion of cloud droplets: Its robustness with respect to key cloud properties, *Atmospheric
Chemistry and Physics*, 15(4), pp. 2009–2017. doi:10.5194/acp-15-2009-2015, 2015.
- 525 WANG Fei, LU Chunsong.: Advances of Theoretical, Observational, and Numerical Studies on Relative Dispersion of
Cloud Droplet Spectral (in China). *Plateau Meteorology*. DOI: 10. 7522/j. issn. 1000-0534. 00067, 2022.



- Wang, F. et al.: An airborne study of the aerosol effect on the dispersion of cloud droplets in a drizzling marine stratocumulus cloud over eastern China, *Atmospheric Research*, 265, p. 105885. doi:10.1016/j.atmosres.2021.105885, 2022.
- 530 Wang, X. et al.: A study of shallow cumulus cloud droplet dispersion by large eddy simulations, *Acta Meteorologica Sinica*, 25(2), pp. 166–175. doi:10.1007/s13351-011-0024-9, 2011.
- Wang, Y. et al.: An observational study on cloud spectral width in North China, *Atmosphere*, 10(3), p. 109. doi:10.3390/atmos10030109, 2019.
- Wang, Y. et al.: Diverse dispersion effects and parameterization of relative dispersion in urban fog in eastern China, *Journal of Geophysical Research: Atmospheres*, 128(6). doi:10.1029/2022jd037514, 2023.
- 535 Wehbe, Y., Temimi, M. and Adler, R.F.: Enhancing precipitation estimates through the fusion of weather radar, satellite retrievals, and surface parameters, *Remote Sensing*, 12(8), p. 1342. doi:10.3390/rs12081342, 2020.
- Xie, X. N., Liu, X. D., & Wang, Z. S.: Research Progress on the Impact of Cloud Droplet Spectrum Dispersion on Aerosol Indirect Effects (in China). *Journal of Earth Environment*, 6(2), 8. DOI: 10.7515/JEE201502008, 2015.
- 540 Xie, X. et al.: Sensitivity study of cloud parameterizations with relative dispersion in CAM5.1: Impacts on aerosol indirect effects, *Atmospheric Chemistry and Physics*, 17(9), pp. 5877–5892. doi:10.5194/acp-17-5877-2017, 2017.
- Yang, F. et al.: Evaluation of multiple forcing data sets for precipitation and shortwave radiation over major land areas of China, *Hydrology and Earth System Sciences*, 21(11), pp. 5805–5821. doi:10.5194/hess-21-5805-2017, 2017.
- Yang, S. et al.: Effects of aerosol number concentration and updraft velocity on relative dispersion during the collision–coalescence growth stage of warm clouds, *Atmosphere*, 14(5), p. 828. doi:10.3390/atmos14050828, 2023.
- 545 Yin, Y. et al.: The effects of giant cloud condensation nuclei on the development of precipitation in convective clouds — a numerical study, *Atmospheric Research*, 53(1–3), pp. 91–116. doi:10.1016/s0169-8095(99)00046-0, 2000.
- YU Guohang, YANG Suying, HU Cheng-rong, et al.: Simulation on Impacts of Aerosol Number Concentration on Physical Characteristics of Warm Clouds during Different Growth Stages [J]. *Journal of Meteorology and Environment*, 38(3): 52–64, 2022.
- 550 Yum, S.S. and Hudson, J.G.: Adiabatic predictions and observations of cloud droplet spectral broadness, *Atmospheric Research*, 73(3–4), pp. 203–223. doi:10.1016/j.atmosres.2004.10.006, 2005.
- Zhao, C. and Ishizaka, Y.: Modeling marine stratocumulus with a detailed microphysical scheme, *Advances in Atmospheric Sciences*, 21(1), pp. 61–74. Available at: <https://doi.org/10.1007/bf03342546>, 2004.
- 555 Zhao, C. et al.: Aircraft measurements of cloud droplet spectral dispersion and implications for indirect aerosol radiative forcing, *Geophysical Research Letters*, 33(16). doi:10.1029/2006gl026653, 2006.
- Zheng, X. et al.: Comparison of macro- and microphysical properties in precipitating and non-precipitating clouds over Central-eastern China during warm season, *Remote Sensing*, 14(1), p. 152. doi:10.3390/rs14010152, 2021.

<https://doi.org/10.5194/egusphere-2023-2644>

Preprint. Discussion started: 12 March 2024

© Author(s) 2024. CC BY 4.0 License.



560 ZHU Lei, LU Chunsong, GAO Sinan, YUM Seong Soo.: Spectral Width of Cloud Droplet Spectra and Its Impact Factors in
Marine Stratocumulus[J]. Chinese Journal of Atmospheric Sciences, 44(3): 575-590. doi: 10.3878/j.issn.1006-
9895.1905.19115, 2020.